Nucleon Resonances: Study of Their Properties through Photo Pion Production

C. Fernández-Ramírez[1,2], E. Moya de Guerra[1,3], and J. M. Udías[3]

[1] Instituto de Estructura de la Materia, CSIC. Serrano 123, E-28006 Madrid, Spain
[2] Departamento de Física Atómica, Molecular y Nuclear. Universidad de Sevilla. Apdo. 1065, E-41080 Sevilla, Spain
[3] Departamento de Física Atómica, Molecular y Nuclear. Facultad de Ciencias Físicas. Universidad Complutense de Madrid. Avda. Complutense s/n, E-28040 Madrid, Spain

Abstract. We present an effective Lagrangian model of the pion photoproduction reaction that we have recently elaborated. We also present a reliable technique to assess the parameters of the nucleon resonances and results on the quadrupole deformation of the $\Delta(1232)$.

1 Introduction

In the last years a great experimental and theoretical effort has been paid to meson production from the nucleon in order to study the properties of the low-lying nucleon resonances and to assess their parameters. This research is achieved through the excitation of the resonances by means of photonic or electronic probes and the study of their decays into mesons (mainly pions) [1]. These parameters are predicted by several theoretical models of the nucleon and their resonances – quark models [2, 3], skyrme models [4], Lattice Quantum Chromodynamics (QCD) [5, 6] – and have to be extracted from experiments through reaction models. The extraction of the parameters (masses, widths, electromagnetic coupling constants, ...) of the nucleon excitations from experimental data has become important in order to assess their properties and to compare with hadron models. The comparison of theoretical predictions from nucleonic models to the results from reaction models provides a guide to improve hadron models and to discriminate among them. Together with pion scattering on the nucleon, single pion photoproduction is the most used mechanism to study the low-lying baryon spectrum. The quantity and quality of the experimental database [7] has been significantly improved thanks to the extensive experimental programs carried out at LEGS (Brookhaven, USA) [8] and MAMI (Mainz, Germany) [9–11]. In this Proceeding we present an outlook of the pion photoproduction model that we have recently elaborated [12,13] based upon an effective Lagrangian approach (ELA) and the technique we have applied to assess the parameters of the nucleon resonances. We also provide some results, and among them results on the quadrupole deformation of the $\Delta(1232)$.

2 Pion Photoproduction

The differential cross section for the $\gamma N \to \pi N$ reaction (Figure 1) can be written in the center of mass reference system as:

$$\frac{d\sigma}{d\Omega_\pi^*} = \frac{1}{64\pi^2} \frac{1}{s^*} \frac{k^*}{E_\gamma^*} \overline{|\mathcal{M}|^2}. \tag{1}$$
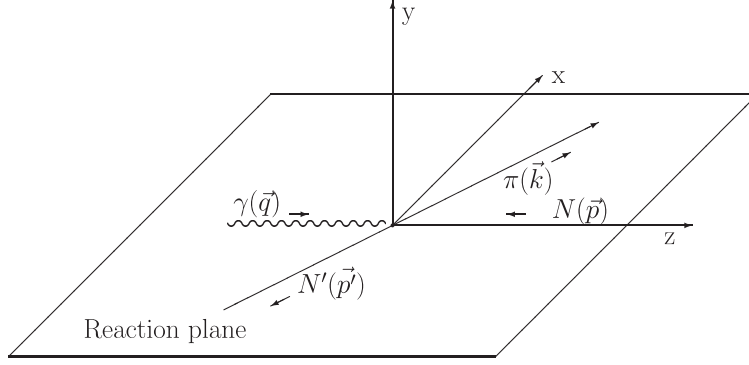
Figure 1. Kinematics of the pion photoproduction process.

The transition probability is:

$$\overline{|\mathcal{M}|^2} = \frac{1}{4} \sum_{\lambda_1 \lambda_2 \lambda_\gamma} |\mathcal{A}_{\lambda_1 \lambda_2 \lambda_\gamma}|^2, \tag{2}$$

where $\mathcal{A}_{\lambda_1 \lambda_2 \lambda_\gamma}$ is the invariant amplitude, with photon polarization λ_γ, initial nucleon helicity λ_1, and final nucleon helicity λ_2. Because of parity, among the eight helicity amplitudes, only four of them are independent:

$$H_N = \mathcal{A}_{\frac{1}{2},-\frac{1}{2},1} = -\mathcal{A}_{-\frac{1}{2},\frac{1}{2},-1}, \tag{3}$$

$$H_{SF} = \mathcal{A}_{-\frac{1}{2},-\frac{1}{2},1} = \mathcal{A}_{\frac{1}{2},\frac{1}{2},-1}, \tag{4}$$

$$H_{SA} = \mathcal{A}_{\frac{1}{2},\frac{1}{2},1} = \mathcal{A}_{-\frac{1}{2},-\frac{1}{2}-1}, \tag{5}$$

$$H_D = \mathcal{A}_{-\frac{1}{2},\frac{1}{2},1} = -\mathcal{A}_{\frac{1}{2},-\frac{1}{2},-1}. \tag{6}$$

Subindices stand for: N, non-spin flip; SF, spin flip with photon and initial nucleon having parallel spins; SA, spin flip with photon and initial nucleon having antiparallel spins; and D, double spin flip.

If we are able to calculate these four invariant amplitudes we can calculate any physical observable (differential cross sections, asymmetries, electromagnetic multipoles, ...). Therefore, the key point to study pion photoproduction is the construction of a reaction model which allows to calculate the invariant amplitudes and
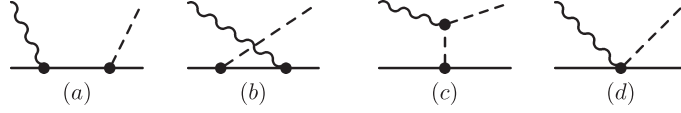
Figure 2. Feynman diagrams for Born terms: (a) s channel, (b) u channel, (c) t channel, and (d) Kroll-Rudermann.

relate the results on physical observables to the intrinsic properties of the involved particles. We have developed a model based upon effective Lagrangians and we provide an outlook in next section. With these Lagrangians we calculate the Feynman diagrams in Figures 2 and 3 and we obtain the invariant amplitudes.

3 The Pion Photoproduction Model

In [12, 13] we have developed a pion photoproduction model up to 1 GeV of photon energy based upon effective Lagrangians. In what follows we provide a brief description of the model. In addition to Born (Figure 2) and vector meson exchange terms (ρ and ω, diagram (e) in Figure 3), the model includes all the four star resonances in Particle Data Group (PDG) [14] up to 1.7 GeV mass and up to spin-3/2: $\Delta(1232)$, N(1440), N(1520), $\Delta(1620)$, N(1650), and $\Delta(1700)$ — diagrams (f) and (g) in Figure 3. Born terms are calculated using the Lagrangian:

$$
\begin{aligned}
\mathcal{L}_{Born} = & -ieF_1^V \hat{A}^\alpha \epsilon_{jk3} \pi_j \left(\partial_\alpha \pi_k\right) - e\hat{A}^\alpha F_1^V \bar{N}\gamma_\alpha \frac{1}{2}\left(F_1^{S/V} + \tau_3\right)N \\
& -ieF_1^V \frac{f_{\pi N}}{m_\pi}\hat{A}^\alpha \bar{N}\gamma_\alpha \gamma_5 \frac{1}{2}[\tau_j, \tau_3]\pi_j N \\
& -\frac{ie}{4M}F_2^V \bar{N}\frac{1}{2}\left(F_2^{S/V} + \tau_3\right)\gamma_{\alpha\beta}N F^{\alpha\beta} + \frac{f_{\pi N}}{m_\pi}\bar{N}\gamma_\alpha\gamma_5\tau_j N\left(\partial^\alpha \pi_j\right),
\end{aligned}
\tag{7}
$$

where e is the absolute value of the electron charge, $f_{\pi N}$ the pion nucleon coupling constant, $F_j^V = F_j^p - F_j^n$ and $F_j^S = F_j^p + F_j^n$ are the isovector and isoscalar nucleon form factors, $F^{\mu\nu} = \partial^\mu \hat{A}^\nu - \partial^\nu \hat{A}^\mu$ is the electromagnetic field ($\hat{A}^\mu$ stands for the photon field), N the nucleon field, and π_j the pion field. The coupling to the pion has been chosen pseudovector in order to ensure the correct low energy behavior and parity.
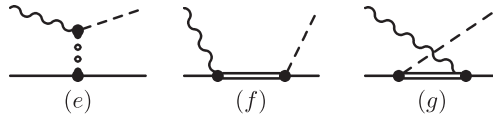
Figure 3. Feynman diagrams for vector meson exchange (e) and resonance excitations: (f) s channel and (g) u channel.

The main advantages of our model compared to previous ones resides on the treatment of resonances. In particular, we avoid some pathologies in the Lagrangians of the spin-3/2 resonances (such as $\Delta(1232)$), present in previous models, implementing a modern approach due to Pascalutsa [15]. Under this approach the (spin-3/2 resonance)-nucleon-pion and the (spin-3/2 resonance)-nucleon-photon vertices have to fulfill the condition $q_\alpha \mathcal{O}^{\alpha\cdots} = 0$ where q is the four-momentum of the spin-3/2 particle, α the vertex index which couples to the spin-3/2 field, and the dots stand for other possible indices. In particular, we write the simplest interacting (spin-3/2 resonance)-nucleon-pion Lagrangian as [15]

$$\mathcal{L}_{int} = -\frac{h}{f_\pi M^*} \bar{N} \epsilon_{\mu\nu\lambda\beta} \gamma^\beta \gamma^5 \left(\partial^\mu N_j^{*\nu}\right) \left(\partial^\lambda \pi_j\right) + \text{H.c.}, \tag{8}$$

where H.c. stands for hermitian conjugate, h is the strong coupling constant, $f_\pi = 92.3$ MeV is the leptonic decay constant of the pion, M^* the mass of the resonance, and π_j, N, and $N_j^{*\nu}$, the pion, nucleon, and spin-3/2 fields respectively.

The model also displays chiral symmetry, gauge invariance, and crossing symmetry. The dressing of the resonances is considered by means of a phenomenological width which takes into account decays into one π, one η, and two π. The width is built in order to fulfill crossing symmetry and contributes to both s and u channels of the resonances.

For the numerical calculations we include form factors for Born terms and vector mesons, in order to regularize the high energy behaviour of these terms we choose form factors as suggested by Davidson and Workman [16] that allow to fulfill gauge invariance and crossing symmetry:

$$\begin{aligned}\hat{F}_B(s,u,t) =& F(s) + F(u) + G(t) - F(s)F(u) - F(s)G(t) - F(u)G(t) \\ & + F(s)F(u)G(t),\end{aligned} \tag{9}$$

where

$$F(l) = \left[1 + \left(l - M^2\right)^2 / \Lambda^4\right]^{-1}, \quad l = s, u; \tag{10}$$

$$G(t) = \left[1 + \left(t - m_\pi^2\right)^2 / \Lambda^4\right]^{-1}. \tag{11}$$

For vector mesons we adopt $\hat{F}_V(t) = G(t)$ with the change $m_\pi \to m_V$. In order to have as few free parameters as possible in the numerical calculations we use the same Λ for both vector mesons and Born terms.

We assume that the final state interactions (FSI) factorize and can be included through the distortion of the πN final state wave function. A detailed calculation of the distortion would require one to calculate higher order pion loops or to develop a phenomenological potential FSI model. The first approach is overwhelmingly complex and the second would introduce additional model-dependencies, which are to be avoided in the present analysis, in as much as we are concerned here with the bare properties of the resonances. We rather include FSI in a phenomenological way by

adding a phase δ_{FSI} to the electromagnetic multipoles. We determine this phase so that the total phase of the electromagnetic multipole is identical to the one of the energy dependent solution of SAID [7]. In this way we are able to disentangle the electromagnetic vertex from FSI effects.

In order to obtain a reliable set of electromagnetic coupling constants of the nucleon resonances we have fitted the experimental electromagnetic multipoles using modern minimization techniques based upon genetic algorithms. In next section we explain the fitting procedure.

4 Fitting Procedure

In order to assess the parameters of the model we had to minimize the function χ^2 defined by

$$\chi^2 = \sum_{j=1}^{m} \left[\frac{\mathcal{M}_j^{exp} - \mathcal{M}_j^{th}(\lambda_1, \ldots, \lambda_n)}{\Delta \mathcal{M}_j^{exp}} \right]^2 , \qquad (12)$$

where $\mathcal{M}^{exp}$ stands for the current energy independent extraction of the multipole analysis of SAID up to 1 GeV for E_{0+}, M_{1-}, E_{1+}, M_{1+}, E_{2-}, and M_{2-} multipoles in the three isospin channels $I = \frac{3}{2}, p, n$ for the $\gamma p \to \pi^0 p$ process [7]. $\Delta \mathcal{M}^{exp}$ is the error and $\mathcal{M}^{th}$ is the multipole given by the model which depends on the parameters $\lambda_1, \ldots, \lambda_n$, which stand for the electromagnetic coupling constans of the resonances and the cutoff Λ. The masses and the widths of the resonances have been taken from the multichannel analysis of Vrana, Dytman, and Lee [17]. Electromagnetic multipoles are complex quantities and we have taken into account 763 data for the real part of the multipoles and the same amount for the imaginary part. Thus, $m = 1526$ data points have been used in the fits.

We have decided to fit electromagnetic multipoles instead of any other physical observable for two reasons mainly. The first one is that electromagnetic multipoles are more sensitive to coupling properties than are other observables so any deficiency in the model shows up much more clearly. The second is that all the observables can be expressed in terms of the multipoles, thus, if the multipoles are properly fitted by the model, so should be the other observables.

In order to fit the data and determine the best parameters of the resonances we have written a genetic algorithm combined with the E04FCF routine from NAG libraries [18]. Although genetic algorithms are computationally more expensive than other algorithms, in a minimization problem it is much less likely for them to get stuck at local minima than for other methods, namely gradient based minimization methods. Thus, in a multiparameter minimization like the one we face here it is probably the best possibility to search for the minimum [12, 19].

Our minimization strategy is as follows:

1. First, the genetic algorithm has been run 400 generations. The first generation is compound by individuals randomly generated within the reasonable values of the parameters. We do not really need so many generations, but we preferred

to let the algorithm run more generations than necessary in order to ensure convergence.

2. When the 400 generations have been run, we use the genetic algorithm solution as the initial value for the E04FCF routine from NAG libraries [18]. We use this routine for fine tunning. The E04FCF routine implements an algorithm that allows to find an unconstrained minimum of a sum of square

$$\text{Minimize } F(x_1, \ldots, x_n) = \sum_{j=1}^{m} |f_j(x_1, \ldots, x_n)|^2, \qquad (13)$$

of m nonlinear functions in n variables ($m \geq n$). This algorithm does not require to know derivatives. From a starting point $x_1^{(1)}$, ..., $x_n^{(1)}$ (in our case supplied by the genetic algorithm) the routine applies a Quasi-Newton method in order to reach the minimum. This method uses a finite-difference approximation to the Hessian matrix to define the search direction. It is a very accurate and fast converging algorithm once we have an initial solution close to the minimum we seek. Therefore, it is perfect for our fine tunning purpouse. If we try to solve our optimization problem by means of the E04FCF routine alone it shows completely useless and no reliable results are obtained because it gets stuck in the first local minimum found.

3. We store the solution and we start again with a different seed for the initial population of the genetic algorithm. After thirty runs of the minimization code, we have thirty different minima. We use them to get new ranges $(\lambda_j^{max}, \lambda_j^{min})$ for the parameters. With these new ranges we start again and repeat the process until we find that all the χ^2 divided by χ^2_{min} are close to unity.

In Figure 4 we provide a sample of the fits to the electromagnetic multipoles that we obtain.

5 Quadrupole Deformation of the Δ(1232)

An important issue that can be studied through pion photoproduction from the nucleon is the existence of a quadrupole deformation in its first excited state, the Δ(1232). Within the quark model, a single spin flip is the standard picture for the photoexcitation of the nucleon into a Δ(1232). If we assume spherically symmetric ($L = 0$) radial wave functions of both parent and daughter, an E2 transition cannot take place, and therefore, a non-vanishing E2 multipolarity evokes a deformed nucleon picture [20].

Over the last few years much effort has been invested in the determination of quadrupole deformation in the nucleon [1, 21]. Because the spin of the nucleon is 1/2, a possible intrinsic quadrupole deformation is not directly observable and its study requires research on its lowest-lying excitation – Δ(1232) – and its decay through pion emission. Hints on the possible deformation will be deduced via the E2/M1 Ratio (EMR).
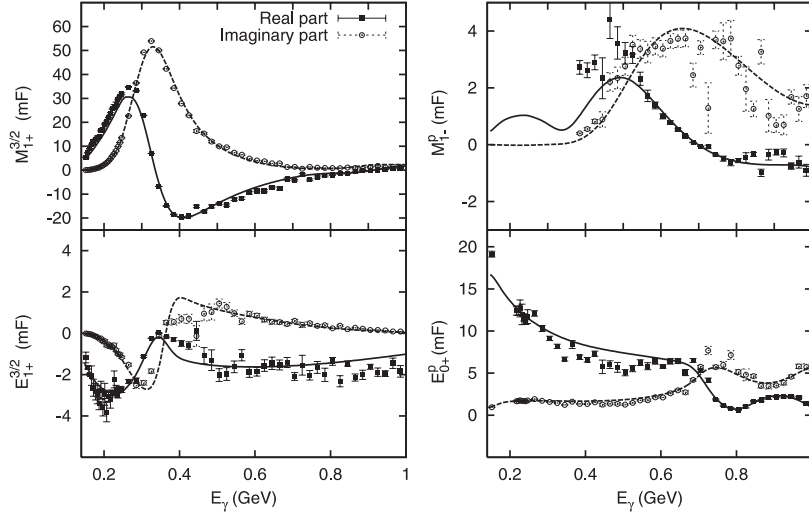
Figure **4.** Electromagnetic multipoles. Curve conventions: solid, real part of the multipole; dashed, imaginary part of the multipole.

Caution must be taken with the various definitions of EMR employed in the literature. We should distinguish between the *intrinsic* (or *bare*) EMR of the $\Delta(1232)$ and the directly measured value which is often called *physical* or *dressed* EMR value [23, 24] and which is obtained as the ratio between the imaginary parts of $E_{1+}^{3/2}$ and $M_{1+}^{3/2}$ at the E_γ value at which $\mathrm{Re}\left[M_{1+}^{3/2}\right] = 0 = \mathrm{Re}\left[E_{1+}^{3/2}\right]$. Since all the reaction models are fitted to the experimental electromagnetic multipoles, they generally reproduce the physical EMR value. We obtain

$$\mathrm{EMR}^{\mathrm{physical}} = \frac{\mathrm{Im}\left[E_{1+}^{3/2}\right]}{\mathrm{Im}\left[M_{1+}^{3/2}\right]} \times 100\% = (-3.9 \pm 1.1)\,\%. \tag{14}$$

However, this measured EMR value is not easily computed with the theoretical models of the nucleon and its resonances. Instead, in order to compare to models of nucleonic structure, it is better to extract the *bare* EMR value of $\Delta(1232)$ which is defined as:

$$\mathrm{EMR}^{\mathrm{bare}} = \frac{G_E^{\Delta(1232)}}{G_M^{\Delta(1232)}} \times 100\%, \tag{15}$$

This depends only on the intrinsic characteristics of the $\Delta(1232)$ and can thus be compared directly to predictions from nucleonic models. It is not, however, directly measurable but must be inferred (in a model dependent way) from reaction models. The intrinsic quadrupole deformation of the $\Delta(1232)$ is found to be EMR= $(-1.30 \pm 0.52)\,\%$, indicative of a small oblate deformation. In Table 1 we compare our EMR values (bare and physical) to the ones extracted by other authors

Table **1.** Comparison of EMR values from nucleonic models and EMR values extracted from data predicted through several reaction models.

Physical EMR, experiments	EMR	Ref.
LEGS Collaboration (Brookhaven)	$(-3.07 \pm 0.26 \pm 0.24)\,\%$	[8]
A1 Collaboration (Mainz)	$(-2.28 \pm 0.29 \pm 0.20)\,\%$	[10]
A2 Collaboration (Mainz)	$(-2.74 \pm 0.03 \pm 0.30)\,\%$	[11]
Particle Data Group (World average)	$(-2.5 \pm 0.5)\,\%$	[14]
Physical EMR, reaction models	EMR	Ref.
Fuda and Alharbi	-2.09%	[22]
Pascalutsa and Tjon	$(-2.4 \pm 0.1)\%$	[23]
Sato and Lee	-2.7%	[24]
Fernández-Ramírez *et al.*	$(-\mathbf{3.9} \pm \mathbf{1.1})\,\%$	[25]
Bare EMR, reaction models	EMR	Ref.
Pascalutsa and Tjon	$(3.8 \pm 1.6)\%$	[23]
Sato and Lee	-1.3%	[24]
Davidson *et al.*	-1.45%	[26]
Garcilazo and Moya de Guerra	-1.42%	[27]
Vanderhaeghen *et al.*	-1.43%	[28]
Fernández-Ramírez *et al.*	$(-\mathbf{1.30} \pm \mathbf{0.52})\,\%$	[25]
Bare EMR, nucleonic models	EMR	Ref.
Non-relativistic quark model	0%	[2]
Constituent quark model	-3.5%	[3]
Skyrme model	$(-3.5 \pm 1.5)\%$	[4]
Lattice QCD (Leinweber *et al.*)	$(3 \pm 8)\%$	[5]
Lattice QCD (Alexandrou *et al.*)		[6]
$\quad(Q^2 = 0.1\ \mathrm{GeV}^2,\, m_\pi = 0)$	$(-1.93 \pm 0.94)\%$	
$\quad(Q^2 = 0.1\ \mathrm{GeV}^2,\, m_\pi = 370\ \mathrm{MeV})$	$(-1.40 \pm 0.60)\%$	

using other models for pion photoproduction, as well as to predictions of nucleonic models. This extraction reconciles results from experiments (physical EMR) with the ones obtained using Lattice QCD (bare EMR) within a consistent and sound framework.

Acknowledgments

References

1. B. Krusche and S. Schadmand, *Prog. Part. Nucl. Phys.* **51**, 399 (2003).
2. C. M. Becchi and G. Morpurgo, *Phys. Lett.* **17**, 352 (1965).
3. A. J. Buchmann, E. Hernández, and A. Faessler, *Phys. Rev. C* **55**, 448 (1997).
4. A. Wirzba and W. Weise, *Phys. Lett. B* **188**, 6 (1987).
5. D. B. Leinweber, T. Draper, and R. M. Woloshyn, *Phys. Rev. D* **48**, 2230 (1993).
6. C. Alexandrou, Ph. de Forcrand, H. Neff, J. W. Negele, W. Schroers, and A. Tsapalis, *Phys. Rev. Lett.* **94**, 021601 (2005).
7. R. A. Arndt, W. J. Briscoe, I. I. Strakovsky, and R. L. Workman, *Phys. Rev. C* **66**, 055213 (2002), SAID database, `http://gwdac.phys.gwu.edu`.
8. G. Blanpied *et al.*, *Phys. Rev. C* **64**, 025203 (2001).
9. C. Molinari *et al.*, *Phys. Lett. B* **371**, 181 (1996);
   J. Peise *et al.*, *Phys. Lett. B* **384**, 37 (1996);
   R. Beck *et al.*, *Phys. Rev. Lett.* **78**, 606 (1997);
   F. Wissmann *et al.*, *Nucl. Phys. A* **660**, 232 (1999).
10. S. Stave *et al.*, `arXiv:nucl-ex/0604013`, (2006).
11. J. Ahrens *et al.*, *Eur. Phys. J. A* **21**, 323 (2004).
12. C. Fernández-Ramírez, *Electromagnetic production of light mesons*, PhD Thesis Dissertation (2006), Universidad Complutense de Madrid.
13. C. Fernández-Ramírez, E. Moya de Guerra, and J. M. Udías, *Ann. Phys. (N.Y.)* **321**, 1408 (2006).
14. W.-M. Yao *et al.*, J. Phys. G **33**, 1 (2006), `http://pdg.lbl.gov`.
15. V. Pascalutsa, *Phys. Rev. D* **58**, 096002 (1998);
    V. Pascalutsa and R. Timmermans, *Phys. Rev. C* **60**, 042201(R) (1999).
16. R. M. Davidson and R. Workman, *Phys. Rev. C* **63**, 058201 (2001);
    R. M. Davidson and R. Workman, *Phys. Rev. C* **63**, 025210 (2001).
17. T. P. Vrana, S. A. Dytman, and T.-S. H. Lee, *Phys. Rep.* **328**, 181 (2000).
18. Numerical Algorithms Group Ltd., Wilkinson House, Jordan Hill Road, Oxford OX2-8DR, UK, `http://www.nag.co.uk/`.
19. D. G. Ireland, S. Janssen, and J. Ryckebusch, *Nucl. Phys. A* **740**, 147 (2004).
20. S. L. Glashow, *Physica A* **96**, 27 (1979).
21. A. M. Bernstein, *Eur. Phys. J. A* **17**, 349 (2003).
22. M. G. Fuda and H. Alharbi, *Phys. Rev. C* **68**, 064002 (2003).
23. V. Pascalutsa and J. A. Tjon, *Phys. Rev. C* **70**, 035209 (2004).
24. T. Sato and T.-S. H. Lee, *Phys. Rev. C* **63**, 055201 (2001).
25. C. Fernández-Ramírez, E. Moya de Guerra, and J. M. Udías, *Phys. Rev. C* **73**, 042201(R) (2006).
26. R. M. Davidson, N. C. Mukhopadhyay, and R. S. Wittman, *Phys. Rev. D* **43**, 71 (1991).
27. H. Garcilazo and E. Moya de Guerra, *Nucl. Phys. A* **562**, 521 (1993).
28. M. Vanderhaeghen, K. Heyde, J. Ryckebusch, and M. Waroquier, *Nucl. Phys. A* **595**, 219 (1995).